Maximum Likelihood Synchronization for Pulse Position Modulation with Inter-Symbol Guard Times

Ryan Rogalin
Jet Propulsion Laboratory
California Institute of Technology
Pasadena, CA 91109, USA
ryan.rogalin@jpl.nasa.gov

Meera Srinivasan
Jet Propulsion Laboratory
California Institute of Technology
Pasadena, CA 91109, USA
meera.srinivasan@jpl.nasa.gov

***Abstract*—Deep space optical communications promises orders of magnitude growth in communication capacity, supporting high data rate applications such as video streaming and high-bandwidth science instruments. Pulse position modulation is the modulation format of choice for deep space applications, and by inserting inter-symbol guard times between the symbols, the signal carries the timing information needed by the demodulator. Accurately extracting this timing information is crucial to demodulating and decoding this signal. In this paper we propose a low complexity maximum likelihood timing estimator for pulse position modulation with inter-symbol guard times which significantly outperforms the prior art in this domain. We show that this estimator can achieve the same performance as prior estimators with an order of magnitude less signal flux, or multiple orders of magnitude less flux-accumulation time. Further we show that this estimator achieves the Cramér-Rao bound, making it asymptotically efficient. This method does not require an explicit synchronization sequence, freeing up channel resources for data transmission.**

I. Introduction

Deep space optical communications promises orders of magnitude higher capacities than radio frequency communications while reducing the mass and power requirements on spacecraft [1]. One method of representing digital information in this regime is pulse position modulation (PPM), where information is encoded in one of M time slots to denote a binary sequence of length $\log_2 M$. Clearly, being able to resolve the correct time slot in which a pulse was transmitted is crucial to the operation of a PPM system, and in order to do so, an estimate of the timing offset at the receiver must be made.

The method of timing estimation described in this paper exploits the use of inter-symbol guard times (ISGTs) to infer this relative timing offset. Inter-symbol guard times are likely to be used in optical PPM communication systems since doing so reduces hardware constraints by eliminating the possibility of back-to-back laser pulses [2]. Because there are no signal pulses transmitted during these ISGTs, the identification of the timing offset may be made by determining the time slots during which no signal pulses are present.

The primary contribution of this paper is a low-complexity maximum-likelihood timing estimator for PPM+ISGT optical links. Existing timing estimators of PPM+ISGT photon counting detectors exploit first moment properties of the arrival process, but do not make claims of optimality [2]. Maximum likelihood results for multipulse PPM (MPPM) and overlapping PPM (OPPM) are known, but they report high complexity and the OPPM method relies on the existence of a primary synchronization which occurs before slot synchronization [3], [4]. General maximum likelihood estimators of optical pulse arrival times are also known [5], but they are not directly useful for communication synchronization due to their complexity. A novel coding-theoretic based method has also been presented [6], but it relies on an explicit sequence for synchronization. The maximum likelihood scheme presented in this report is of $\mathcal{O}(M)$ complexity, yet achieves the Cramer-Rao bound even in relatively low flux scenarios. Further, the approach outlined in this paper can be utilized with an explicit synchronization sequence as well as using just the data itself (data-driven synchronization). This is particularly important in low flux scenarios, in which transmitting a sufficiently long synchronization sequence may severely impact the data throughput.

II. Model

The synchronization schemes outlined in this paper assume the use of pulse position modulation with an inter-symbol guard time. In conventional PPM, information is encoded in the timing position of an optical pulse. For a symbol of length T_{sym}, the symbol is divided into M slots of length $T_{slot} = T_{sym}/M$, and messages of length $\log_2 M$ are encoded by sending an optical pulse in one of the M slots. With the addition of an ISGT, the symbol is divided into $M + P$ slots of length $T_{slot} = T_{sym}/(M + P)$, and messages of length

This publication was prepared by the Jet Propulsion Laboratory, California Institute of Technology, under a contract with the National Aeronautics and Space Administration.

$\log_2 M$ are encoded by sending an optical pulse in one of the first M slots, while the remaining P slots do not contain signal pulses. Note that the selection of the parameter P depends upon a combination of synchronization requirements, hardware constraints and data rates, and is outside the scope of this paper.

We assume the use of an optical detector assembly which provides the number of photo-electon counts per given time interval. The output process of such a detector is well-modeled as a Poisson point process whose mean number of counts is proportional to the incident light on the detector [7]. This mean number of counts may be non-linearly proportional to the incident light due to phenomena such as blocking [8]. We observe the detector process $x[n]$ over N symbols, and assume a single sample per slot is measured. For Poisson distributed counts, the sum of the counts per slot provides a sufficient statistic for the timing offset, justifying the use of a single sample per slot. In practice, samples are summed over the slot duration to generate the single slot statistic. Thus the indices of $x[n]$ range in $n \in \{0, \ldots, (M+P)N-1\}$. The time over which we collect counts, or the integration time, is given by $T_{int} = N(M+P)T_{slot}$. The variable N may be increased to collect signal flux for a sufficient amount of time in order to be able to distinguish signal slots from ISGT slots. The observations are binned into a vector $\mathbf{y}$ such that $y_m = \sum_{i=0}^{N-1} x[m+i(M+P)]$ with $m \in \{0, \ldots, M+P-1\}$. In the following analysis we assume that there is no frequency offset (or equivalently that the frequency offset is known). However, in concordance with other works [2], this algorithm can still operate in the presence of unknown frequency offsets by adjusting the integration time N.

With no timing offset and conditioned on there not being a signal pulse in slot n, the distribution of the observation $x[n]$ is Poisson with parameter K_b, the mean number of background photon counts per slot. With no timing offset and conditioning on there being a signal pulse in slot n, the distribution of the observation $x[n]$ is Poisson with parameter $K_s + K_b$, where K_s is the mean number of signal photon counts per symbol. The condition of knowing whether the slot contains or does not contain a signal pulse is akin to knowing the transmitted pulse sequence (e.g. observing a known training sequence). In this case, because the elements of $\mathbf{y}$ are deterministic sums of Poisson random variables, they are also Poisson distributed. In the case where the symbols are unknown, the elements of $\mathbf{y}$ are no longer Poisson distributed since the number of summed signal slots is now random, as will be discussed in Section V. Assuming that the signal slots are deterministically uniform (i.e. that the same number of pulses appear in each signal slot over the duration of the integration time), then there are $\frac{N}{M}$ aggregated pulses in $y[m]$ for $m \in \{0, \ldots, M-1\}$. Note that this is also true if the particular pulse sequence is unknown, but the number of pulses in each position is deterministically uniform. The aggregate observation vector is then Poisson distributed with parameter $\frac{N}{M}K_s + NK_b$ for $m \in \{0, \ldots, M-1\}$ and Poisson distributed with parameter NK_b for $m \in \{M, \ldots, M+P-1\}$.

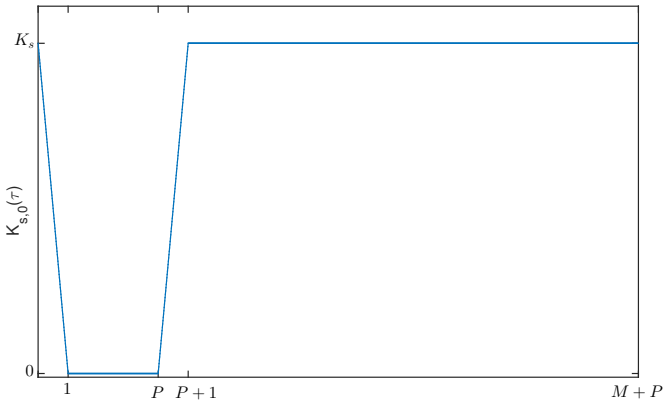

Fig. 1. Arrival rate function for the first aggregate slot, y_0 as a function of the timing offset τ.

In the presence of a timing offset τ the distribution of the observation vector changes. Let $X \sim \text{Poi}(r)$ denote that X is a Poisson random variable with mean r. If τ is integer-valued, then the distributions of the elements of $\mathbf{y}$ are cyclically shifted by τ (e.g., if $\tau = 1$, then $y_m \sim \text{Poi}(\frac{N}{M}K_s + NK_b)$ for $m \in \{1, \ldots, M\}$ and $y_m \sim \text{Poi}(NK_b)$ for $m \in \{M+1, \ldots, M+P-1, 0\}$. If τ contains a fractional component then the means of the two slots adjacent to the ISGT are scaled between the count and background parameters. Decomposing the timing offset into integer and fractional components k and ϵ, respectively, we observe that

$$y_m \sim \begin{cases} \text{Poi}((1-\epsilon)\frac{N}{M}K_s + NK_b) & m = k \bmod (M+P) \\ \text{Poi}(\frac{N}{M}K_s + NK_b) & m \in \{k+1, \ldots, k+M-1\} \bmod (M+P) \\ \text{Poi}(\epsilon\frac{N}{M}K_s + NK_b) & m = (k+M) \bmod (M+P) \\ \text{Poi}(NK_b) & m \in \{k+M+1, \ldots, k+M+P-1\} \bmod (M+P). \end{cases} \tag{1}$$

Alternatively, we can write the probability mass function of each slot given a timing offset using an intensity function $\lambda_m(\tau)$ which varies with τ:

$$P_{Y_m|\tau}(y_m|\tau) = \frac{\lambda_m(\tau)^{y_m} e^{-\lambda_m(\tau)}}{y_m!}. \tag{2}$$

The intensity function can be written as

$$\lambda_m(\tau) = \frac{N}{M}K_{s,m}(\tau) + NK_b \tag{3}$$

where $K_{s,m}(\tau)$ is the mean signal count in the mth slot in the presence of a timing offset τ. The effective signal count of the first aggregate slot y_0 is shown in Figure 1. Subsequent

effective count functions can be written as cyclic shifts of this function, such that $\lambda_m(\tau) = \lambda_0((\tau - m) \bmod (M+P))$.

III. Pilot-Aided Maximum Likelihood Synchronization

Given the probability mass function of the aggregate observation vector $\mathbf{y}$ given τ, we can form the log likelihood function:

$$\ell(\tau;\mathbf{y}) = \log \prod_{m=0}^{M+P-1} P_{Y_m|\tau}(y_m|\tau) \tag{4}$$

$$= \sum_{m=0}^{M+P-1} \log P_{Y_m|\tau}(y_m|\tau) \tag{5}$$

$$= \sum_{m=0}^{M+P-1} y_m \log \lambda_0((\tau - m) \bmod (M+P)) - \lambda_0((\tau - m) \bmod (M+P)) - \log(y_m!) \tag{6}$$

$$= \sum_{m=0}^{M+P-1} y_m \log \lambda_0((\tau - m) \bmod (M+P)) + C \tag{7}$$

where C is a constant. We wish to maximize this likelihood function with respect to τ, yet we observe that it is not differentiable at integer values due to the piecewise definition of $\lambda_m(\tau)$. However, on each open integer interval $(j, j+1)$, the likelihood function is both differentiable and concave (since it forms a sum of concave functions of affine functions [9]).

Taking the partial derivative with respect to τ over the interval $(j, j+1)$, we derive

$$\frac{\partial}{\partial \tau}\ell(\tau;\mathbf{y}) = \frac{y_{j+M}\frac{N}{M}K_s}{(\tau - j)\frac{N}{M}K_s + NK_b} - \frac{y_j \frac{N}{M}K_s}{(j+1-\tau)\frac{N}{M}K_s + NK_b} \tag{8}$$

$$= 0 \tag{9}$$

where the indices of the elements of $\mathbf{y}$ are taken modulo $M+P$. Solving for τ results in the estimate

$$\widehat{\tau}_{\text{ML},j} = \frac{\frac{N}{M}K_s((j+1)y_{j+M} + jy_j) + NK_b(y_{j+M} - y_j)}{\frac{N}{M}K_s(y_{j+M} + y_j)}. \tag{10}$$

If the estimate $\widehat{\tau}_{\text{ML},j}$ is less than j, then we let $\widehat{\tau}_{\text{ML},j} = j$, and if $\widehat{\tau}_{\text{ML},j}$ is greater than $j+1$, then we let $\widehat{\tau}_{\text{ML},j} = j+1$. As such, the maximum likelihood estimate can be found by evaluating the $M+P$ quantities $\widehat{\tau}_{\text{ML},j}$ for $j \in \{0, \ldots, M+P-1\}$, then choosing the overall estimate as

$$\widehat{\tau}_{\text{ML}} = \arg\max_{\widehat{\tau}_{\text{ML},j}} \ell(\widehat{\tau}_{\text{ML},j};\mathbf{y}). \tag{11}$$

Thus the timing estimate can be formed by calculating $2(M+P)$ simple algebraic equations and evaluating a maximum over $M+P$ quantities. An example of the log likelihood function can be seen in Figure 2, in which $M = 16$ and $P = 4$, and where the timing offset is $\tau = 14.4545$. The circles denote the maxima on each integer interval, and the maximum of the overall function can be seen to lie approximately at 14.4545.

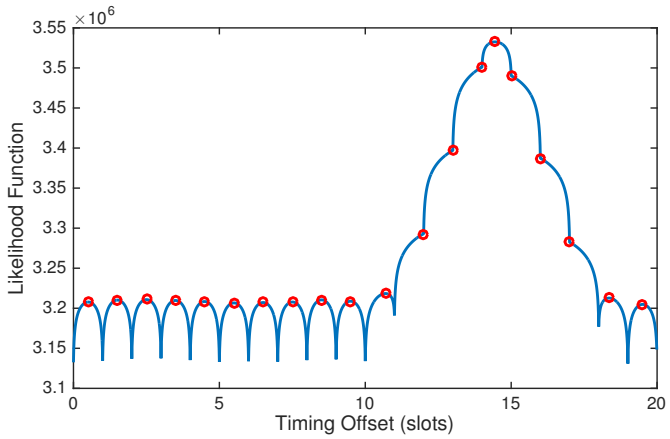

Fig. 2. The log likelihood function for an example with modulation order $M = 16$ and intersymbol guard length $P = 4$ slots. The actual timing offset is $\tau = 14.4545$ slots. Each red circle identifies the maximum on that integer interval.

To provide a basis for performance evaluation, we compare the root mean square error of the ML estimator to that of a correlation-based method [2]. The correlation method utilizes the same slot count measurements as the ML method. It assumes a single slot is used for the ISGT, so the smallest slot count corresponds to the integer estimate of the timing offset:

$$\widehat{k}_{\text{corr}} = \arg\min_j y_j. \tag{12}$$

The fractional timing offset estimate is then formed from the two adjacent count statistics:

$$\widehat{\epsilon}_{\text{corr}} = \frac{y_{\widehat{k}-1} - y_{\widehat{k}+1}}{\frac{N}{M}K_s}. \tag{13}$$

Since the ML method works for an arbitrary size ISGT, a slight modification to the correlation method is necessary to perform a fair comparison between the methods. For $P > 1$ and assuming that $M + P \bmod P = 0$, we accumulate the slot counts of the P adjacent bins to form a "superslot" count vector $\mathbf{z}$ of length $\frac{M+P}{P}$, i.e. $z_j = \sum_{i=0}^{P-1} y_{jP+i}$. The correlation-superslot method then forms the integer and fractional estimates of the timing offset as:

$$\widehat{k}_{\text{corr-ss}} = P \arg\min_j z_j. \tag{14}$$

and

$$\widehat{\epsilon}_{\text{corr-ss}} = P\frac{z_{\widehat{k}-1} - z_{\widehat{k}+1}}{\frac{N}{M}PK_s}. \tag{15}$$

Finally, we also consider a hybrid scheme which forms the integer estimate from the correlation-superslot method, and the

TABLE I
THE EXAMPLE SCENARIOS FOR WHICH THE TIMING ESTIMATION PERFORMANCE IS SIMULATED

	Scenario 1	Scenario 2
M	16	128
P	4	32
N	10^5	1.25×10^5
T_{slot}	0.5 ns	5 ns
K_s	0.25	0.09
K_b	0.00005	0.001

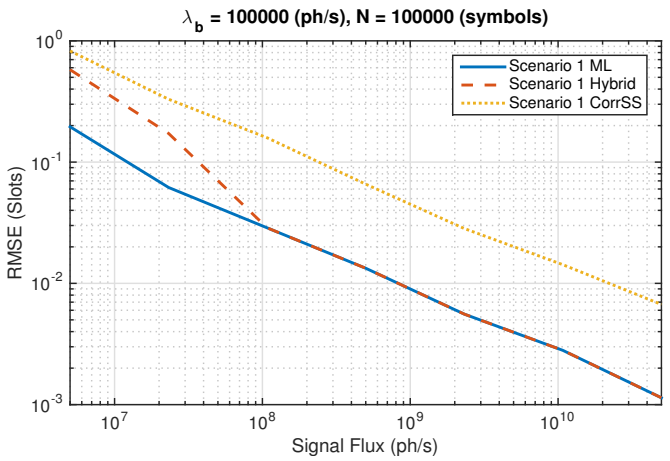

Fig. 3. Root mean square error performance of the three estimation schemes for Scenario 1 in the presence of Poisson distributed data as in (1). For this scenario, the Hybrid scheme can be seen matching the ML.

overall estimate using the ML estimate for that particular bin:

$$\widehat{k}_{\text{hybrid}} = P \arg\min_j z_j. \tag{16}$$

and

$$\widehat{\tau}_{\text{hybrid}} = \widehat{\tau}_{\text{ML},\widehat{k}}. \tag{17}$$

We will observe the performance of these schemes for two scenarios, the parameters of which are described in Table I. The first scenario utilizes a low order PPM with moderate signal flux, while the second scenario utilizes higher order PPM with low signal flux and comparatively high background flux. These scenarios simulate high-rate near-Earth, and low-rate deep-space channels, respectively.

The performance of the three schemes in terms of root mean squared error is shown in Figure 3 for Scenario 1. Data is generated using the Poisson model outlined in (1) for random timing offsets τ. As can be seen, the performance of the hybrid scheme approaches that of the ML with increasing flux.

IV. Timing Estimate Cramer-Rao Bound

To quantify how optimal these estimators are with respect to mean squared error, we can derive the Cramér-Rao lower bound (CRB) on the estimation variance. We note that strictly speaking, the non-differentiability of the likelihood function means the CRB does not exist at integer-valued timing offsets. However, because it is differentiable at non-integer values and the probability of observing an integer-valued timing offset is zero, it may still prove useful as a performance metric. Further, for the numeric quantities utilized in this paper ($\tau = 4.5$), the likelihood function (and thus the CRB) exists. We begin by calculating the Fisher information:

$$\mathcal{I}(\tau) = -\mathbb{E}\left[\frac{\partial^2}{\partial \tau^2}\ell(\tau; \mathbf{y})\right] \tag{18}$$

$$= -\mathbb{E}\left[\frac{\partial^2}{\partial \tau^2}\sum_{m=0}^{M+P-1}\log\left(P_{Y_m|\tau}(y_m|\tau)\right)\right]. \tag{19}$$

The second derivative of the likelihood function is non-zero for two values of m: $m_1 = \lfloor \tau \rfloor$ and $m_2 = \lfloor \tau \rfloor + M$ (where again these indices are taken modulo $M+P$). Then the Fisher information may be written:

$$\mathcal{I}(\tau) = \mathbb{E}\left[\frac{K_s^2 y_{m_1}}{(K_s(1-\epsilon)+K_bM)^2} + \frac{K_s^2 y_{m_2}}{(K_s\epsilon + K_bM)^2}\right] \tag{20}$$

$$= \frac{K_s^2\left(\frac{N}{M}K_s(1-\epsilon)+NK_b\right)}{(K_s(1-\epsilon)+K_bM)^2} + \frac{K_s^2\left(\frac{N}{M}K_s\epsilon+NK_b\right)}{(K_s\epsilon+K_bM)^2} \tag{21}$$

$$= \frac{K_s^2\left(\frac{N}{M}K_s + 2NK_b\right)}{\epsilon(1-\epsilon)K_s^2 + MK_sK_b + M^2K_b^2}. \tag{22}$$

Finally, the CRB is defined as:

$$\text{CRB}(\tau) = \mathcal{I}(\tau)^{-1} \tag{23}$$

$$= \frac{\epsilon(1-\epsilon)K_s^2 + MK_sK_b + M^2K_b^2}{K_s^2\left(\frac{N}{M}K_s + 2NK_b\right)}. \tag{24}$$

It is worth noting that the CRB of the timing estimator decreases as $\mathcal{O}(K_s^{-1})$ and $\mathcal{O}(N^{-1})$, in concordance with similar estimates in the AWGN channel, which fall as $\mathcal{O}(\text{SNR}^{-1})$ and $\mathcal{O}(N^{-1})$ [10]. As can be seen in Figure 4, the maximum likelihood scheme is asymptotically efficient. Since the CRB is dependent upon the timing offset (specifically, it is dependent upon the fractional component of the timing offset), a deterministic value ($\tau = 4.5$) was chosen for the results in Figure 4 to make a meaningful comparison.

V. Data-Driven PPM Synchronization

When the sequence of transmitted pulses is unknown or is not deterministically uniform, the aggregated slot counts are no longer Poisson distributed. This is the case when the data sequence is used for synchronization without additional pilots, as is sometimes done in RF OFDM communications by exploiting the cyclostationarity of the cyclic prefix [11]. Assuming the pulses are uniformly randomly distributed in the M signal-containing slots, we can calculate the aggregate slot count pmf of the signal component explicitly. Let $K_m \sim \text{Binomial}(N, \frac{1}{M})$ be a random variable denoting the number of times a signal appears in the mth slot over N symbols.

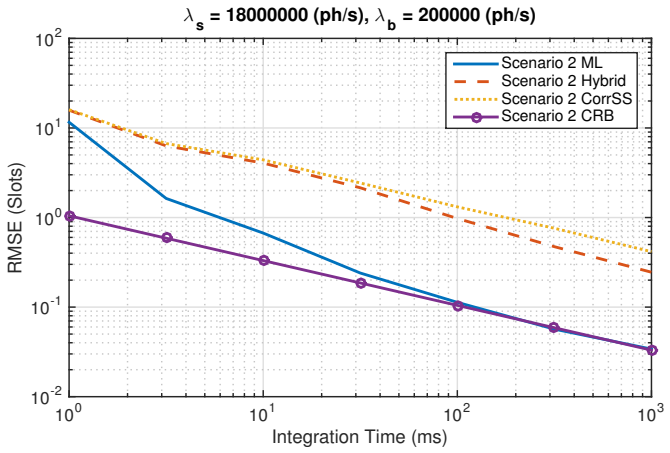

Fig. 4. Root mean square error performance of the three estimation schemes with Scenario 2 and the Cramer-Rao bound. In this scenario the ML scheme achieves the CRB with significantly less integration time (with sufficiently long integration time, the Hybrid scheme will match the ML). These simulations used a timing offset $\tau = 4.5$ slots.

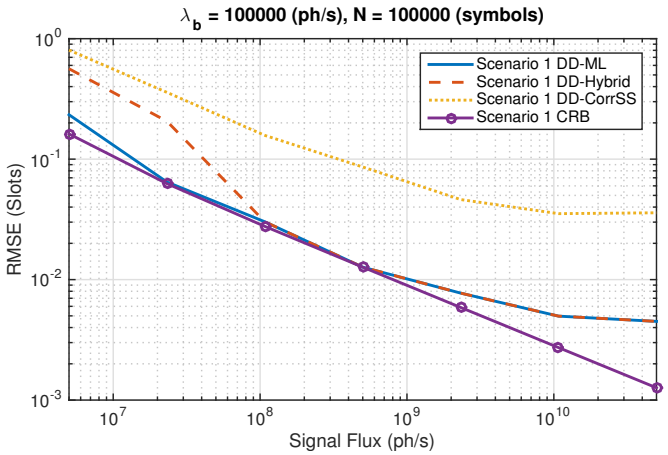

Fig. 5. Performance of the three schemes with Scenario 1 when using the mismatched pmf corresponding to unknown, uniformly distributed PPM pulses. The saturation of the RMSE occurs at high signal flux, but can be combatted with longer integration times.

Then

$$\begin{aligned} P_{Y_m|\tau}(y_m|\tau) &= \mathbb{P}\left(\sum_{j=0}^{N-1} X[m+jN] = y_m \middle| \tau\right) \\ &\overset{(a)}{=} \mathbb{P}\left(\sum_{j=0}^{K_m-1} X[m+jN] \right. \\ &\qquad \left. + \sum_{j=K_m}^{N-1} X[m+jN] = y_m \middle| \tau\right) \\ &\overset{(b)}{=} \sum_{k=0}^{N} \mathbb{P}(K_m = k)\mathbb{P}\left(\sum_{j=0}^{k-1} X[m+jN] \right. \\ &\qquad \left. + \sum_{j=k}^{N-1} X[m+jN] = y_m \middle| \tau\right) \end{aligned} \tag{25}$$

where in (a) we have utilized the fact that, without loss of generality, we may assume the K_m signal-containing slots to be in the first K_m symbols, and in (b) we have utilized the law of total probability. By definition, the Binomial random variable yields

$$\mathbb{P}(K_m = k) = \binom{N}{k}\left(\frac{1}{M}\right)^k\left(1-\frac{1}{M}\right)^{N-k} \tag{26}$$

and the Poisson yields

$$\mathbb{P}\left(\sum_{j=0}^{k-1} X[m+jN] + \sum_{j=k}^{N-1} X[m+jN] = y_m\right) = \frac{(kK_{s,m}(\tau)+NK_b)^{y_m}\exp(-(kK_{s,m}(\tau)+NK_b))}{y_m!}. \tag{27}$$

We note that even though the individual slot counts are Poisson distributed (for a given τ), the distribution of aggregate slot counts is not Poisson since the mean and variance are not the same. From the law of total variance, the variance of this distribution can be calculated explicitly:

$$\begin{aligned} \text{var}[Y_m|\tau] &= \mathbb{E}_K\left[\text{var}_{Y_m|K}\left[Y_m|K,\tau\right]\right] + \\ &\qquad \text{var}_K\left[\mathbb{E}_{Y_m|K}\left[Y_m|K,\tau\right]\right] \\ &= \mathbb{E}_K\left[KK_{s,m}(\tau)+NK_b\right] + \\ &\qquad \text{var}_K\left[KK_{s,m}(\tau)+NK_b\right] \\ &= \frac{N}{M}K_{s,m}(\tau) + NK_b + K_{s,m}(\tau)^2\frac{N}{M}\left(1-\frac{1}{M}\right) \end{aligned} \tag{28}$$

This distribution is much less tractable than the Poisson distribution, and a closed-form solution of the ML scheme is unlikely. Instead of deriving another ML scheme for the above distribution, we will inspect the performance of the ML scheme derived in Section III in the presence of aggregate slot counts given by the actual distribution in (25). We note the resulting RMSE performance of this mismatched scheme in Figure 5. The RMSE exhibits an "error floor" behavior in which increasing the signal flux does not decrease the MSE of the timing estimator. This is in sharp contrast to the ideal Poisson distributed counts, in which increasing the signal flux results in better estimator performance.

To confirm this effect and to dispel any suspicion that this error floor is merely an artifact of simulation, we derive a closed form expression of the MSE of the correlation-superslot method using the bias-variance decomposition:

$$\text{MSE}(\widehat{\tau}) = \text{var}(\widehat{\tau}) + \text{bias}(\widehat{\tau})^2. \tag{29}$$

In particular, we assume we are operating in a high $\frac{K_s}{K_b}$ regime, such that correct detection of the ISGT is possible (i.e. $\widehat{k} = k$).

The correlation-superslot method can be easily shown to be unbiased:

$$\begin{aligned}\mathbb{E}[\widehat{\epsilon}] &= \mathbb{E}\left[\frac{Y_{k-1}-Y_{k+1}}{N/MK_s}\right] \\ &= \frac{\frac{N}{M}K_s + NK_b - (1-\epsilon)\frac{N}{M}K_s - NK_b}{\frac{N}{M}K_s} \\ &= \epsilon. \end{aligned} \tag{30}$$

Thus the MSE of the estimator is equal to its variance. The variance can be similarly found:

$$\begin{aligned}\text{var}(\widehat{\epsilon}) &= \mathbb{E}\left[\frac{(Y_{k-1}-Y_{k+1})^2}{(\frac{N}{M}K_s)^2}\right] - \epsilon^2 \\ &= \frac{1}{\frac{N^2}{M^2}K_s^2}\big(\text{var}(Y_{k-1}) + \mathbb{E}[Y_{k-1}]^2 + \text{var}(Y_{k+1}) \\ &\quad +\mathbb{E}[Y_{k+1}]^2 - 2\mathbb{E}[Y_{k-1}]\mathbb{E}[Y_{k+1}]\big) - \epsilon^2. \end{aligned} \tag{31}$$

When the aggregate slot counts are Poisson distributed (as in Section III, in which a pilot sequence is used), then

$$\text{MSE}(\widehat{\epsilon}_{\text{pilot}}) = \frac{M(2-\epsilon)}{NK_s} + \frac{M^2K_b}{NK_s^2}. \tag{32}$$

By contrast, when the observed sequence is unknown and the observed counts are subject to the additional variance derived in (28), the MSE is

$$\text{MSE}(\widehat{\epsilon}_{\text{data}}) = \frac{M(2-\epsilon)}{NK_s} + \frac{2M^2K_b}{NK_s^2} + (1+(1-\epsilon)^2)\frac{M-1}{N}. \tag{33}$$

The difference between these two regimes is readily apparent; whereas the pilot-driven MSE follows

$$\lim_{K_s\to\infty} \text{MSE}(\widehat{\epsilon}_{\text{pilot}}) = 0, \tag{34}$$

the data-driven MSE tends toward

$$\lim_{K_s\to\infty} \text{MSE}(\widehat{\epsilon}_{\text{data}}) = (1-(1-\epsilon)^2)\frac{M-1}{N}. \tag{35}$$

However, the MSEs in both cases are proportional to N^{-1}, meaning that this "error floor" can be overcome with longer integration times. In practice, the error floor is only apparent at high signal powers, and the low-flux scenarios in which PPM would be utilized will not be impacted by this phenomenon.

VI. Conclusion

In this paper we have shown the existence of a low complexity maximum likelihood estimator for optical PPM+ISGT that outperforms previously known schemes with minor additional computational complexity. For the scenarios presented (which model deep space links) the estimator is show to outperform the best known prior approach by roughly an order of magnitude in RMSE. Furthermore, unlike methods which do not have an inter-symbol guard time, the method outlined here can be utilized without an explicit synchronization sequence.

References

[1] H. Hemmati, *Deep Space Optical Communications*, ser. JPL Deep-Space Communications and Navigation Series. Wiley, 2006. [Online]. Available: https://books.google.com/books?id=Cj52X7jK5OgC

[2] K. Quirk, J. Gin, and M. Srinivasan, "Optical PPM synchronization for photon counting receivers," in *Military Communications Conference, 2008. MILCOM 2008. IEEE*, Nov 2008, pp. 1–7.

[3] R. Velidi and C. N. Georghiades, "Symbol synchronization for optical multi-pulse pulse position modulation systems," in *Personal Wireless Communications, 1994., IEEE International Conference on*, Aug 1994, pp. 182–184.

[4] S. Patarasen and C. N. Georghiades, "Maximum-likelihood symbol synchronization and detection of OPPM sequences," *IEEE Transactions on Communications*, vol. 42, no. 6, pp. 2282–2290, Jun 1994.

[5] B. Erkmen and B. Moision, "Maximum likelihood time-of-arrival estimation of optical pulses via photon-counting photodetectors," in *Information Theory, 2009. ISIT 2009. IEEE International Symposium on*, June 2009, pp. 1909–1913.

[6] Y. Fujiwara, "Self-synchronizing pulse position modulation with error tolerance," *IEEE Transactions on Information Theory*, vol. 59, no. 9, pp. 5352–5362, Sept 2013.

[7] R. Gagliardi and S. Karp, *Optical Communications*, ser. Wiley Series in Telecommunications and Signal Processing. Wiley, 1995. [Online]. Available: https://books.google.com/books?id=ySAfAQAAIAAJ

[8] D. F. Yu and J. A. Fessler, "Mean and variance of single photon counting with deadtime," *Physics in Medicine and Biology*, vol. 45, no. 7, p. 2043, 2000.

[9] S. Boyd and L. Vandenberghe, *Convex Optimization*. New York, NY, USA: Cambridge University Press, 2004.

[10] D. Rife and R. Boorstyn, "Single tone parameter estimation from discrete-time observations," *Information Theory, IEEE Transactions on*, vol. 20, no. 5, pp. 591–598, Sep 1974.

[11] J.-J. van de Beek, M. Sandell, and P. Borjesson, "ML estimation of time and frequency offset in OFDM systems," *Signal Processing, IEEE Transactions on*, vol. 45, no. 7, pp. 1800–1805, Jul 1997.